Inorganic Chemistry

Article

pubs.acs.org/IC

Speciation of La(III) Chloride Complexes in Water and Acetonitrile: A Density Functional Study

Michael Bühl,*[,†] Nicolas Sieffert,[‡] Aurélie Partouche,[‡] Alain Chaumont,[§] and Georges Wipff[§]

[†]School of Chemistry, University of St. Andrews, North Haugh, St. Andrews, Fife KY16 9ST, U.K.

[‡]UMR-5250 CNRS, Département de Chimie Moléculaire, Université Joseph Fourier Grenoble I, BP 53, 38041 Grenoble Cedex 9, France

[§]UMR 7177 CNRS, Laboratoire MSM, Institut de Chimie, 1 rue Blaise Pascal, 67000 Strasbourg, France

Supporting Information

ABSTRACT: Car–Parrinello molecular dynamics (CMPD) simulations and static computations are reported at the BLYP level of density functional theory (DFT) for mixed $[LaCl_x(H_2O)_y(MeCN)_z]^{3-x}$ complexes in aqueous and nonaqueous solution (acetonitrile). Both methodologies predict coordination numbers (i.e., $x + y + z$) that are successively lower than nine as the Cl content increases from $x = 0$ to 3. While the static DFT method with implicit solvation through a polarizable continuum model overestimates the binding strength of chloride and erroneously predicts $[LaCl_2(H_2O)_5]^+$ as global free-energy minimum, constrained CPMD simulations with explicit solvent and thermodynamic integration reproduce the weak binding of chloride in water reasonably well. Special attention is called to the dipole moments of coordinated water molecules as function of coligands and solvent, evaluated through maximally localized Wannier function centers along the CPMD trajectories. Cooperative polarization of these water ligands by the metal cation and the surrounding solvent is remarkably sensitive to fluctuations of the La–O distances and, to a lesser extent, on the La-water tilt angles. The mean dipole moment of water ligands is rather insensitive to the other coligands, oscillating around 3.2 D, 3.5 D, and 3.3 D in MeCN, water, and [dmim]Cl solution, respectively, the latter being an archetypical ionic liquid.

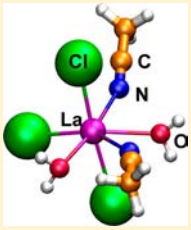

1. INTRODUCTION

Understanding the speciation of metal complexes in water and in non-aqueous solvents is key to controlling their extraction properties. This is particularly important for the rare earth elements, which can be difficult to separate because of their tendency to form three-valent cations with similar chemical characteristics. The separation of lanthanides and actinides is an important issue in nuclear waste reprocessing, where chelating aromatic N-donors are emerging as promising extractants.[1,2] Which complexes are formed in a given solution depends on the mutual affinity between the metal cations and the potential neutral and anionic ligands that are present, governed by their respective solvation free energies. As the latter are vastly different between aqueous, organic, or ionic solvents, a plethora of coordination environments can be realized.[3]

During extraction from the aqueous into an organic phase, the extractant has to displace water ligands from the aquo complexes that are ubiquitous in water. The equilibria that are involved can be delicately balanced by the counterions present. Using static and dynamic density functional theory (DFT) computations, we have recently studied the competition between water and acetonitrile, a prototypical organic N-donor, for coordination to uranyl ion.[4] The preference of water over acetonitrile coordination was found to depend on solvation and on the presence of anionic ligands, specifically chloride, bound to the metal. Cooperative polarization of water ligands by the metal and by H-bonded solvent molecules from the second solvation shell was identified as an important factor in these studies. To probe for the transferability of these findings to other metal complexes, we now report a similar DFT study for the $La^{3+}/H_2O/MeCN/Cl^-$ system, calling special attention to structural preferences as emerging from first-principles molecular dynamics (MD) simulations.

This quaternary system is complex and only partially charted by experiment or theory. In solution, the coordination environment about La can be studied with neutron/X-ray scattering or absorption spectroscopy such as EXAFS.[5] In aqueous solution with noncoordinating counterions (such as perchlorate), it is commonly accepted that La^{3+} exists as nine-coordinate $[La(H_2O)_9]^{3+}$,[3] in accordance with the presence of this ion in numerous solids characterized by X-ray crystallography.[6,7] This ion has also been studied in pure water through Car–Parrinello-MD (CPMD) simulations using the HCTH and the BLYP functionals,[8,9] at the Hartree–Fock level in a QM/MM-MD framework,[10] and in numerous classical MD studies.[11]

In the gas phase, anionic binary $La_nCl_{3n+1}^-$ complexes show a tendency for aggregation into larger oligonuclear clusters.[12] Aqueous lanthanum chloride solutions have been studied with X-ray absorption and/or MD simulations, which point to the preference for nine-coordinated $[LaCl(H_2O)_8]^{2+}$ and eight-coordinated $[LaCl_2(H_2O)_6]^+$ at low[13] and high chloride concentration,[14,15] respectively. For neat molten $LaCl_3$, coordination numbers around eight are obtained through

Received: October 15, 2012
Published: November 26, 2012

   dx.doi.org/10.1021/ic302255a | Inorg. Chem. 2012, 51, 13396–13407

Scheme 1. Labelling of the Investigated Complexes[a]

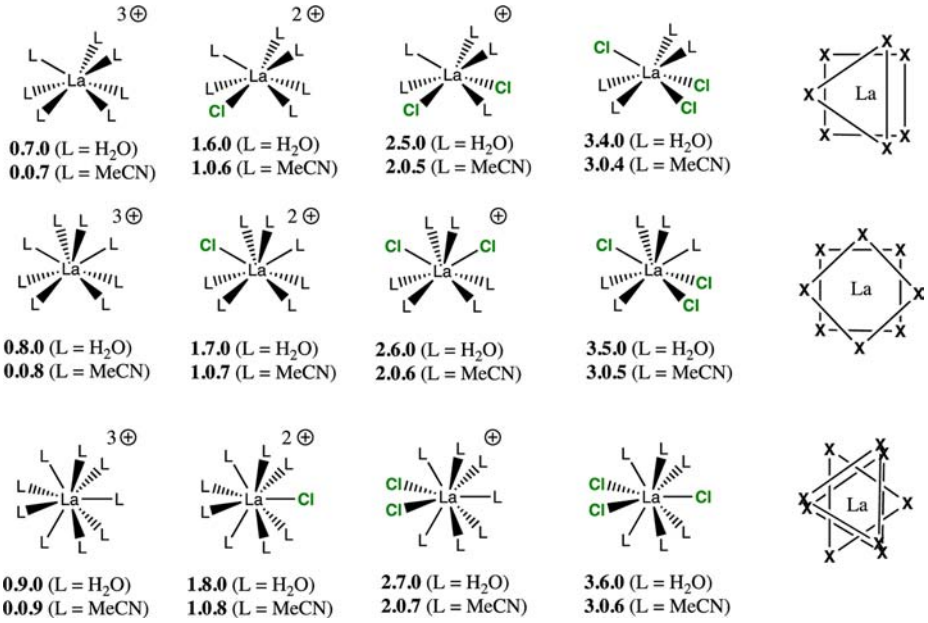

[a]Labelled according to the number of chloro (first digit), aquo (second digit), and acetonitrile ligands (third digit).

Table 1. Solutions of La(III) Complexes Simulated with CPMD[a]

solute	solvent	box size (Å)^3	starting config.	time (ps)[b]
0.9.0	58 H_2O	13 × 13 × 13	X-ray[c]	→**0.8.0**·$\mathbf{H_2O}$
0.9.0·(3Cl^-)	52 H_2O	13 × 13 × 13	X-ray[c]	4.2 (NVE) + 2.0
	35 MeCN	15 × 15 × 15	Amber[d]	→**0.8.0**·$\mathbf{H_2O}$
0.8.0	53 H_2O	13 × 13 × 13	from **0.9.0**	3.0
	35 MeCN	15 × 15 × 15	Amber	(1.5) + 8.5
0.8.0 (3Cl^-)	53 H_2O	13 × 13 × 13	PTI1 end point	3.0
	35 MeCN	15 × 15 × 15	Amber[d]	→ **0.8.1** (3Cl^-)
1.8.0 (2Cl^-)	59 H_2O	13 × 13 × 13	PTI2 end point	1.5 then → **1.7.0**·(2Cl^-)·$\mathbf{H_2O}$
1.7.0 (2Cl^-)	60 H_2O	13 × 13 × 13	from **1.8.0** (2Cl^-)	(1.5) + 3.0
2.6.0 Cl^-	80 H_2O	13.75 × 13.75 × 13.75	Amber[d]	(1.5) + 4.8
	35 MeCN	15 × 15 × 15	from **3.6.0**	(1.5) + 4.2
3.6.0	62 H_2O	13 × 13 × 13	Amber	→**3.5.0**·$\mathbf{H_2O}$
	35 MeCN	15 × 15 × 15	Amber	→**3.3.1 or 2.6.0**·$\mathbf{Cl^-}$[e]
3.5.0	63 H_2O	13 × 13 × 13	from **3.6.0**	2.7
	35 MeCN	15 × 15 × 15	Amber[d]	→**3.4.0**·$\mathbf{H_2O}$
	36 [dmim]Cl	20 × 20 × 20	Amber	1.2
3.3.1···**3** $\mathbf{H_2O}$	35 MeCN	15 × 15 × 15	from **3.6.0**	7.0
3.5.0···**2** $\mathbf{H_2O}$	35 MeCN	15 × 15 × 15	Adapted from **3.4.1**	→ **2.5.0** Cl^- 2 H_2O
3.2.2	35 MeCN	15 × 15 × 15	X-ray[f]	4.8

[a]BLYP functional, 80 Ry cutoff (see Method section for further details and Scheme 1 for labelling of the complexes), number of second-shell chloride counterions are given in parentheses, when present. [b]After 0.5 to 1.5 ps of equilibration. [c]Cation from reference 42, manually placed into solvent box from equilibrated CPMD of $[Co(H_2O)_6]^{3+}$ (from reference 43). [d]The final structure of the complex obtained in water is used as starting structure for the construction of the systems in explicit acetonitrile. [e]**3.4.1**·(**2** $\mathbf{H_2O}$) obtained without constraints, **2.6.0**·$\mathbf{Cl^-}$ after additional CPMD pre-equilibration with constraints, where the differences of La−O distances of two opposite aquo ligands are fixed, as described in reference 4a. [f]Complex from Er analogue, reference 44.

neutron diffraction (ca. 8.2)[16] and classical MD simulations (ca. 7.6).[17]

Mixed La^{3+}/H_2O/MeCN complexes have been studied in the gas phase from electrospray ionization (ESI)-mass spectrometry and DFT calculations, showing a preference for eight-coordination.[18] In the solid, $[La(MeCN)_9]^{3+}$ has been characterized,[19] which has been found to be stable in dry acetonitrile in classical MD simulations.[20] Such simulations have also been used to study the coordination sphere about La^{3+} in imidazolium-based ionic liquids (ILs),[21] an important and highly promising[22] class of nonaqueous solvents. Speciation and La^{3+}-anion interactions in organic solvents have been studied through NMR and IR spectroscopy,[23] although to our knowledge no direct structural information, for example from EXAFS, is available for La complexes in acetonitrile.

It is the purpose of this study to expand our knowledge of structural and energetic properties of La(III) complexes

dx.doi.org/10.1021/ic302255a | Inorg. Chem. 2012, 51, 13396−13407

through first-principles modeling of selected, as yet unexplored islands in the $La^{3+}/H_2O/MeCN/Cl^-$ phase diagram, specifically for aqueous and acetonitrile solutions. Comparison with previous results for the related system based on UO_2^{2+} [4] affords insights into the general affinity of M^{n+} ions toward water in condensed phases as a function of charge and other coligands. We considered a series of seven- to nine-coordinated complexes involving different combinations of chloro, aquo, and acetonitrile ligands (for labeling see Scheme 1).

2. COMPUTATIONAL DETAILS

Similar methods and basis sets as in our uranyl studies were employed.[4] Nonperiodic geometry optimizations were performed in the gas phase using the BLYP[24] functional, the small-core Stuttgart-Dresden relativistic ECP together with its contracted [10s8p5d4f3g] valence basis set on La,[25] standard 6-31G(d,p) basis for all other elements, and a fine integration grid (75 radial shells with 302 angular points per shell), denoted SDD. The minimum character of each stationary point was verified by computation of the harmonic vibrational frequencies, which were all real. To model the changes in entropy for the condensed phase, reflected in the changes between corresponding ΔE and ΔG values (denoted δE_G), the standard expressions from statistical thermodynamics have been evaluated in the gas phase at a pressure of 1354 atm[26] (at T = 298 K). Refined single-point energies were evaluated both in the gas-phase and in a continuum using the PCM implementation of Tomasi and coworkers[27] (employing the united-atom UFF radii and the parameters of acetonitrile and water) at the BLYP/SDD(+) level, that is, using the geometries optimized in the respective medium, the same SDD ECP and valence basis on La, and 6-311+G(d,p) basis[28] on all other elements (the resulting energies in the continuum are denoted E_{solv}). Following the recommendation by Ho, Klamt, and Coote,[29] free energies in solution, ΔG(PCM), have been obtained from $E_{solv} + \delta E_G + \delta G_{nes}$, where G_{nes} denotes the sum of nonelectrostatic contributions, that is, cavitation and dispersion-repulsion interactions.[30] In addition, estimates for the basis-set superposition error (BSSE) of individual bonds were included, which were computed for complex **2.1a** using the Counterpoise method,[31] employing the BLYP functional, SDD(+) basis, and the BLYP/SDD geometry optimized in the continuum. These corrections (denoted E_{BSSE}), are detailed in the Supporting Information, Table S1.

The BLYP functional was chosen for direct comparison with the Car–Parrinello molecular dynamics (CPMD) simulations (see below), which employed it for compatibility with our previous simulations of aqueous solutions,[32] where this functional performs better than most other standard GGAs for describing the properties of liquid water.[33] Selected atomic charges were obtained from Mulliken and natural population analysis (NPA).[34] These calculations were performed with the Gaussian 03[35] suite of programs, except for the NPA charges, which were evaluated with Gaussian 09.[36]

CPMD[37] simulations were performed using the BLYP functional and norm-conserving pseudopotentials that had been generated according to the Troullier and Martins procedure[38] and transformed into the Kleinman-Bylander form.[39] For lanthanum, the semicore (or small-core) pseudopotential was employed that had been generated according to the recommendations in reference 9 (where it is denoted PP1). Periodic boundary conditions were imposed using cubic supercells (see Table 1 for details of the simulated systems). Kohn–Sham orbitals were expanded in plane waves at the Γ-point up to a kinetic energy cutoff of 80 Ry. Simulations were performed in the NVT ensemble using a single Nosé-Hoover thermostat set to 320 K (frequency 1800 cm^{-1}), a fictitious electronic mass of 600 au, and a time step of 0.121 fs. Selected simulations were run with a kinetic energy cutoff of 100 Ry and a time step of 0.073 fs. To maintain the time step, hydrogen was substituted with deuterium. Initial simulations for **0.9.0** were performed in the NVE ensemble, after short pre-equilibration keeping the temperature within 320 ± 50 K through velocity rescaling. The somewhat higher temperature was chosen to increase solvent mobility and improve the sampling. Long-range electrostatic interactions were treated with the Ewald method. Simulations of solutions started either from pre-equilibrated CPMD simulations of related systems (replacing the solute with the La complex) or from pre-equilibrated classical MD snapshots using the AMBER force field[40] (200 ps with frozen solute) and were continued for 3–17 ps in each case; data were collected for analysis during the last picosecond. A short simulation was also performed for **3.5.0** in liquid [dmim]Cl (dmim = 1,3-dimethylimidazolium) at a temperature of 425 K, following the protocol adopted previously.[41] According to the usual indicators (radial distribution functions, diffusion coefficients), the simulated solutions remained liquid-like throughout.

Selected geometries were optimized in the gas phase using the same setup as described above until the maximum gradient was less than 5.10^{-4} a.u (denoted CP-opt). The resulting charge distributions were analyzed by transforming the Kohn–Sham MOs into maximally localized Wannier functions characterized by their centers.[45] For dynamic ensembles, Wannier centers were evaluated for 50 snapshots taken during the last picosecond.

Constrained CPMD simulations were performed along predefined reaction coordinates (bond distances r) connecting complexes with different coordination numbers, to evaluate the change in the Helmholtz free energy by pointwise thermodynamic integration (PTI)[46] of the mean constraint force $\langle f \rangle$ along these coordinates via

$$\Delta A_{a\to b} = -\int_a^b \langle f(r) \rangle \, dr \qquad (1)$$

At each point, the system was propagated until $\langle f \rangle$ was sufficiently converged (usually within 1.5–2 ps after 0.5 ps of equilibration, see the Supporting Information, Figure S1. Each new point was continued from the final, equilibrated configuration of the previous one, using 2000 steps of continuous slow growth to increase the constrained distance. All CP-opt computations and CPMD simulations were performed with the CPMD program.[47]

3. RESULTS AND DISCUSSION

3.1. CPMD Simulations. We begin our discussion with a worked example, the prototypical nonahydrate, **0.9.0**, in water (labelling scheme see Scheme 1). Even though we used the same functional and pseudopotentials as in reference 9, in our hands the pristine trication (i.e., without counterions) was not stable in pure water, but quickly (within less than 0.5 ps)[48] lost one water ligand to afford **0.8.0**. This happened both with cutoffs of 80 and 100 Ry (the latter being close to the 110 Ry that have been used in reference 9)[49] and is probably related to the slightly different setup in both studies (NVE at ca. 320 K with La^{3+} + 67 water in 13 Å box, ρ = 1.0, in this work,[50] versus NVT at 300 K La^{3+} + 64 water in 12.4 Å box, ρ = 1.1, in reference 9).

The apparent instability of pristine **0.9.0** under our simulation conditions may also be related to the general tendency of DFT to underestimate metal–ligand binding energies.[51] Following indications from simulations for uranyl complexes, where explicit inclusion of counterions can enhance the binding strength of weakly bound water ligands,[52] we prepared a solution of **0.9.0** with three chloride ions placed in the second solvation shell (at arbitrary positions in a roughly trigonal array). Although it is difficult to achieve full equilibration within the short time scales accessible, such a contact ion pair is arguably a better model for solutions at high concentrations (≈ 1 M) and/or ionic strengths than pristine **0.9.0** in pure water (which can be taken as a model for high dilution). In any event, **0.9.0**·(3Cl^-) turned out to be (meta)stable in water during several picoseconds (ps) of unconstrained simulation. During the last 2 ps (in the NVT ensemble), the mean La–O distance was 2.65(13) Å, similar to

dx.doi.org/10.1021/ic302255a | Inorg. Chem. 2012, 51, 13396–13407

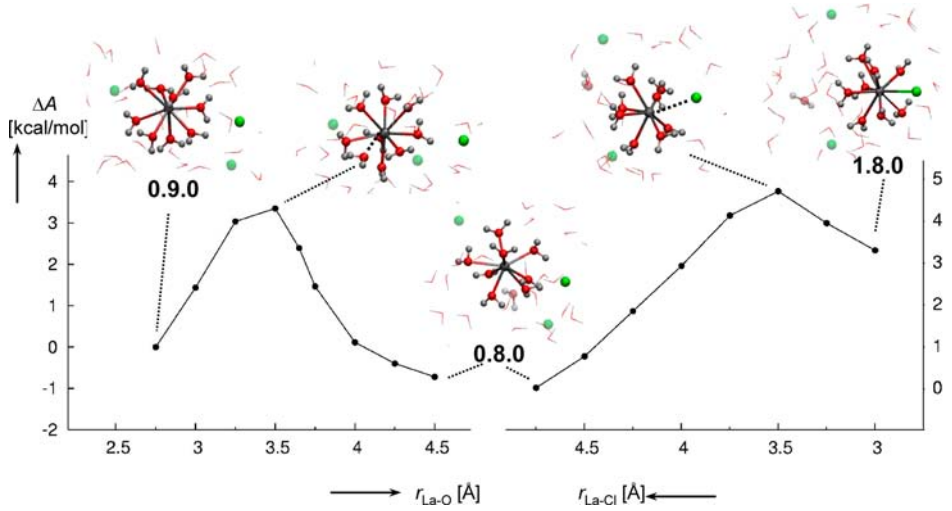

Figure 1. Change in free energy, ΔA, from constrained CPMD simulations and thermodynamic integration, including representative snapshots from the indicated regions; left: dissociation of one water ligand in $[La(H_2O)_9]^{3+}$ (**0.9.0**, reaction coordinate: La−O distance); right: association of one chloride to the resulting **0.8.0** (reaction coordinate: La−Cl distance).

the recent QM/MM-HF value, 2.61 Å,[10] but somewhat longer than the CPMD value reported previously for pristine **0.9.0**, 2.58 Å,[9] or the recent EXAFS-derived range, 2.54 Å−2.56 Å.[53]

Subsequently the preference for eight- vs nine-coordination was probed through thermodynamic integration using one La−O distance as reaction coordinate. The resulting free-energy profile is sketched on the left-hand side of Figure 1. After passing a shallow barrier ($\Delta A^{\ddagger}$ = 3.3 kcal/mol at $r \approx 3.5$ Å), the overall driving force for water dissociation affording **0.8.0**·(**3Cl**$^-$) is ΔA = −0.7 (±0.7) kcal/mol.[54] A slight preference for coordination numbers less than 9 (namely 8.0−8.5) had already be noted in metadynamics simulations of the same system, that is, **0.9.0**·(**3Cl**$^-$),[8] at the CPMD/HCTH level. In view of the accepted nine-coordination of La(III)-hydrate, these findings again indicate the propensity of DFT to underestimate metal−ligand bond strengths. On the other hand, the thermodynamic sink of the nonahydrate cannot be vastly deeper than that of the octahydrate, because the latter has been found in some solids.[7]

To calculate the chloride binding energy of La^{3+}(aq), a quantity that can be compared to experiment, a second path was constructed starting from the last point of the one just discussed (snapshot labeled **0.8.0** in Figure 1). Using the La−Cl distance to the nearest of the three chlorides as reaction coordinate, this ion was pulled toward La to afford **1.8.0**·(**2Cl**$^-$) (see right-hand side of Figure 1). Near the end of this path, the nascent nine-coordinate complex appeared to become increasingly labile, and it was occasionally necessary to freeze the La−O distance to an individual water ligand to prevent its dissociation. When the last point of this path (top right snapshot in Figure 1) was continued with all constraints lifted, the **1.8.0**·(**2Cl**$^-$) complex remained stable for about 1.5 ps, at which point one water ligand dissociated completely, to form **1.7.0**·(**2Cl**$^-$), see the Supporting Information, Figure S2.[55] Before this event, the La−Cl distance averaged to 2.98(10) Å. Using classical Monte Carlo simulations biased to reproduce cross sections from neutron and X-ray scattering experiments, a somewhat shorter distance has been obtained, about 2.8 Å.[13] Interestingly, this technique also pointed to a mean number of coordinated water ligands of about 7.5 under the experimental conditions (1 M aqueous $LaCl_3$ at pH 1), that is, less than 8. Apparently, water is indeed less strongly bound when one Cl^- is coordinated to La^{3+}.

Chloride uptake by **0.8.0** is computed to be endergonic by ΔA = 3.3 (±0.6) kcal/mol, involving a barrier of $\Delta A^{\ddagger}$ = 4.7 kcal/mol at $r \approx 3.5$ Å (right-hand side of Figure 1). The two paths in Figure 1 can be combined into a single reaction describing the displacement of one water ligand by chloride:

$$\textbf{0.9.0}\,(\textbf{3Cl}^-) \rightarrow \textbf{1.8.0}\,(\textbf{2Cl}^-) + H_2O,$$
$$\Delta A = 2.6(\pm 0.9)\ \text{kcal/mol} \qquad (2)$$

From equilibrium constants measured using different techniques and under different conditions (ionic strengths between 1 and 4 M, $\beta_{La,Cl}$ = 0.67 to 1.6 mol dm^{-3}),[13,56] free energies between ΔG = −0.3 to +0.2 kcal/mol can been derived for this reaction. Extrapolation to zero ionic strength has afforded an estimate of log $\beta^0_{La,Cl}$ = 1.43 (±0.12) mol dm^{-3},[56] corresponding to ΔG^0 = 2.0 kcal/mol. Despite the shortcomings of our DFT level discussed above, the CPMD-derived ΔA in eq 2 is in excellent agreement with this value, apparently benefiting from fortuitous error cancellation. CPMD/BLYP simulations are thus indicated to afford reasonable *relative* La^{3+}-ligand binding energies, similar to what had been found for uranyl.[32]

Because of the high computational cost, however, this technique was not applied to the other systems of this study. We performed a few exploratory unconstrained simulations for selected systems (Table 1) to probe for spontaneous processes. Even if the latter are but singular events with little statistical significance, they can give first insights into relative affinities toward different ligands in mixed complexes.[4a] In all solution simulations, overall neutrality of the boxes was afforded by explicitly including the appropriate number of chloride counterions.

In water, **2.6.0**·**Cl**$^-$ remained stable, consistent with the interpretation of EXAFS data[14] and CPMD simulations at the BP86 level.[15] The latter had been performed for a concentrated solution with high ionic strength (1 La^{3+}, 5 Li^+, 7 Cl^- in 30 H_2O). Under these conditions, one associative water exchange had been observed, passing through a transient nine-coordinated **2.7.0** species, which persisted for 2.5 ps. No

dx.doi.org/10.1021/ic302255a | *Inorg. Chem.* 2012, 51, 13396−13407

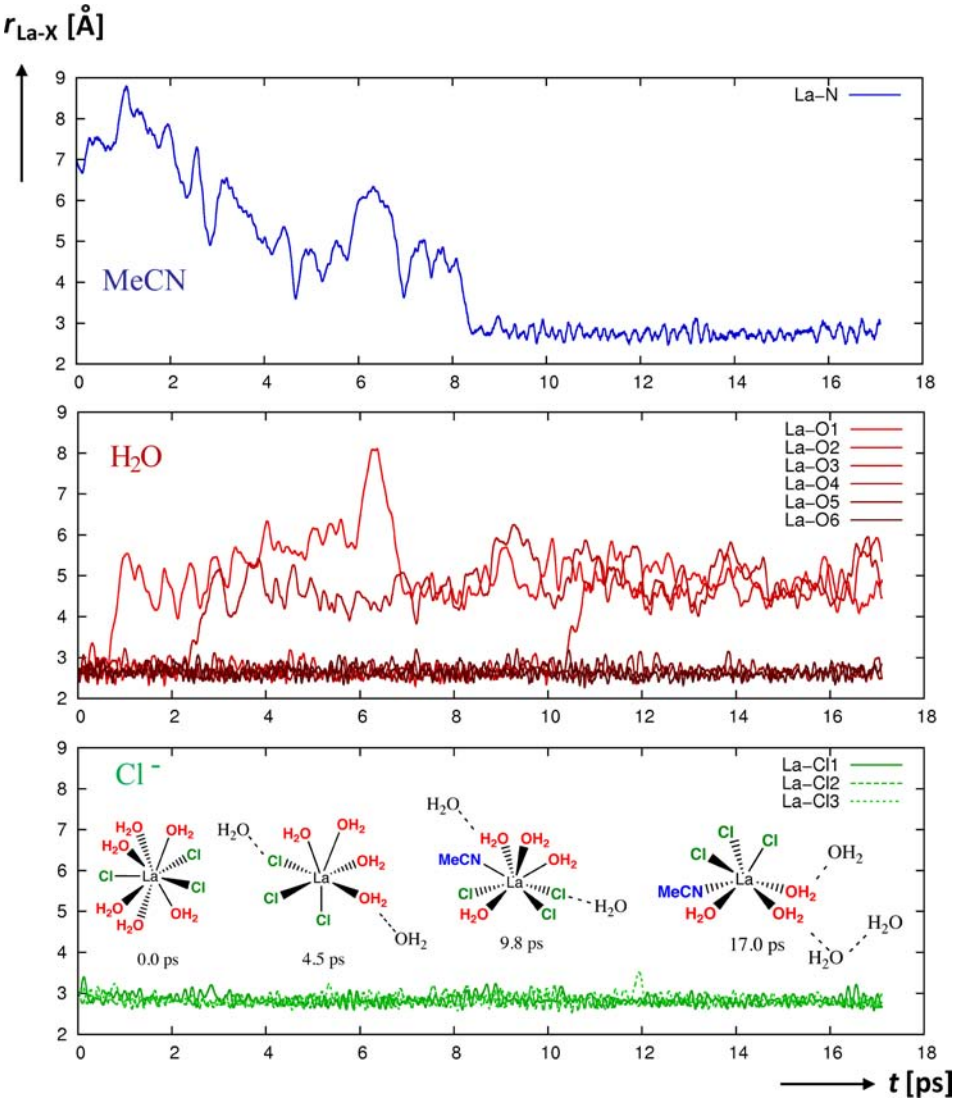

Figure 2. Time evolution (ps) of La-ligand interatomic distances (Å) during a CPMD simulation starting from **3.6.0** in explicit acetonitrile, showing the spontaneous decoordination of two H_2O ligands followed by the coordination of one MeCN molecule to the metal (at $t \approx 8$ ps). At $t \approx 11$ ps, one more H_2O dissociates to afford **3.3.1**.

such exchange was observed in our more dilute system. The mean La−Cl distance, 2.94(12) Å, is close to the EXAFS-derived value, 2.92 Å.[14] The apparent reduction in binding strength to water on going from nine-coordinate La^{3+} to eight-coordinate $LaCl_2^+$ is similar to what had been predicted from CPMD for five-coordinate UO_2^{2+} vs four-coordinate UO_2Cl_2,[57] and subsequently confirmed in a high-energy X-ray scattering study.[58] As expected, **3.6.0** turned out to be instable in water, rapidly (within 1.4 ps) losing one water ligand; the resulting eight-coordinated **3.5.0** proved (meta)stable for the remaining 3.5 ps.

Selected species were also run in acetonitrile (Table 1). With fewer and more sluggish solvent molecules than in the aqueous solutions, the relevance of these short-time simulations may be more limited. Nonetheless, interesting variations were observed on going from water to the organic solvent: **0.9.0**·($3Cl^-$) appeared to be slightly less stable in acetonitrile, where one water dissociated already within 1.4 ps (after 1.5 ps of constrained pre-equilibration), forming the transient **0.8.0** ($3Cl^-$) complex, this is followed by a spontaneous coordination of an acetonitrile molecule, affording **0.8.1**, which remains stable for the remaining 5.4 ps of MD. A similar process occurred when a simulation of **3.6.0** in acetonitrile was started directly from an Amber-pre-equilibrated configuration, two water molecules detached within about 2 ps, affording seven-coordinate **3.4.0** (first part of Figure 2). The latter persisted for about 4.5 ps, when one solvent molecule spontaneously attached to the metal (top of Figure 2), restoring eight-coordination in the resulting **3.4.1**, which after 11 ps lost another water molecule, forming **3.3.1** (Figure 2).

When the CPMD run starting from the same **3.6.0** configuration is preceded by a short (1.5 ps) pre-equilibration with fixed La−Cl and La−O distances, it is one chloride that dissociates spontaneously within 0.6 ps after the constraints are lifted, affording **2.6.0**·Cl^-. Similar "computational experiments" were performed in the case of **3.5.0**: when starting a CPMD simulation from a pre-equilibrated system with constraints, a spontaneous dissociation of one H_2O ligand is observed. When starting another CPMD from a complex **3.5.0** obtained by substituting the coordinated MeCN molecule by H_2O in the transient **3.4.1** complex mentioned below, the spontaneous dissociation of one Cl^- ligand occurred, that is, affording

dx.doi.org/10.1021/ic302255a | Inorg. Chem. 2012, 51, 13396−13407

2.5.0·Cl^- after about 10 ps of MD. No conclusions can be made regarding the relative stabilities of these resulting species, that is, **3.3.1**·(**2** H_2O) vs **2.6.0**·Cl^-(**MeCN**) and **3.4.0** (H_2O) vs **3.4.1** (**3** H_2O), but apparently the nine-coordination is not stable in the tris(chloro) species. A coordination number between seven and eight may be favored (cf. the spontaneous increase in coordination number from seven to eight, followed by a decrease from eight to seven, cf. Figure 2). For a heavier lanthanide, such a mixed complex has been characterized through X-ray crystallography, namely, seven-coordinate $ErCl_3(H_2O)_2(MeCN)_2$.[44,59] The La-analogue, **3.2.2** (Supporting Information, Figure S3) remained seven-coordinate in explicit acetonitrile for up to about 5 ps, without attaching another solvent molecule. From the general tendency toward a decrease of coordination numbers across the lanthanide row, however, a coordination number larger than seven would be expected for La.

As a note on the side, structures with T-shaped $LaCl_3$ units, as found in $ErCl_3(H_2O)_2(MeCN)_2$, are not formed spontaneously in explicit acetonitrile. Even when starting from **3.6.0** with a planar $LaCl_3$ moiety, the chloride ligands move into syn positions with a pyramidal $LaCl_3$ core (see Figure 2). Similarly, no T-shaped isomers are obtained in gas-phase optimizations (see below), because H_2O ligands tend to form bridging Cl···HOH···Cl interactions, dragging the chlorides out of the equatorial plane.[60]

3.2. Dipole Moment Analysis. As in previous CPMD simulations of aqueous La hydrate and chloride complexes, charge distributions were analyzed in terms of localized Wannier functions. Assuming the electronic charge is concentrated in points located on the centers of the Wannier functions (corresponding to electron pairs of bonds or lone pairs), dipole moments of fragments within a molecule or a periodic array of molecules can be calculated.[61] This approach has been used successfully to evaluate the dipole moments of individual water molecules in bulk water,[62] to reproduce the experimental dipole moments of pristine H_2O and MeCN molecules,[4] and to evaluate dipole polarizabilities of a series of ions in aqueous solution.[63] The results are collected in Table 2.

In the static minima in the gas phase, the water dipole moment increases with decreasing coordination number (compare for example, **0.9.0** and **0.8.0** in Table 2), and decreases with increasing chloride content (see series from **0.8.0** to **3.5.0**). As found previously for uranyl complexes,[4] the charge donation from the negative chloride ligands makes the metal center less electrophilic, thus causing less polarization in the other coordinated ligands. This effect is also reflected in the NPA charges of La and O, which become less positive and more negative, respectively, with increasing Cl content (Table 3).

In aqueous solution, the mean dipole moments of water ligands are remarkably similar for all species, at $\mu \approx 3.5$ D (Table 2), about 0.5 D larger than that of bulk water (ca. 3 D).[62] Similar averages had been reported for pristine aqueous **0.9.0**[9] and **2.6.0** in concentrated LiCl,[15] as well as for the related aqueous curium(III) hydrates $[Cm(H_2O)_n]^{3+}$ (n = 8, 9).[64] In acetonitrile, the mean dipole moments is about 0.3 D lower than in water, and tend to decrease slightly when three chlorides are coordinated (compare **0.8.0** vs **3.5.0**).

Possible correlations between selected geometrical parameters and the dipole moments of coordinated water molecules along the trajectories are analyzed in terms of scatter (density) plots shown in Figure 3. Plotting the dipole moment vs the La−O distance reveals that the induced polarization from the metal occurs mainly at very short-range and vanishes very fast as La−O increases. For instance, moving 0.25 Å away from the equilibrium distance leads to a value of μ_{H2O} close to that of water molecules in the bulk (ca. 3.0 D in water), irrespective whether there is no chloride at all (top left in Figure 3), chlorides are present in the second shell (middle left) or coordinated to the metal (bottom left). The same effect is also observed in the case of acetonitrile solutions (see Supporting Information, Figure S4).

Correlating the dipole moment with the La-water tilt angle (i.e., the La−O-M_{HH} angle, where M_{HH} denotes the midpoint between the two H atoms, see Supporting Information, Scheme S1) shows a slight tendency for higher polarization of the H_2O ligands when they are less strongly tilted away from a "linear" coordination mode (where θ_{tilt} would approach 180°),[65] see plot at the bottom of Figure 3. Because there is a slight tendency for smaller tilts at shorter distances (see Supporting Information, Figure S5), this slight angle dependence of μ_{H2O} may actually be related to the distance dependence just discussed. Overall it appears that cooperative polarization

Table 2. Average Dipole Moments (in D) of Aquo Ligands within the Complexes As Obtained from CP-opt in the Gas Phase, and from CPMD in Explicit Water and Acetonitrile (Standard Deviations in Parentheses)

	$\langle\mu_{H2O}\rangle$, D		
	gas phase[a]	in acetonitrile[b]	in water[b]
H_2O[c]	1.84	2.20(12)	~3.0
0.9.0	3.31(3)	3.32(34)	3.44(32)
1.8.0	3.07(6)		3.35(31)
0.8.0	3.48(2)	[3.41(27)][d]	3.59(34) [3.53(35)][d]
1.7.0	3.17(5)		3.56(29)
2.6.0	2.89(3)	3.23(31)	3.52(35)
3.5.0	2.67(3)	3.05(36)	3.49(28)
3.3.1···3 H_2O		3.22(27)[e]	
0.8.1	3.25(3)	3.24(32)	

[a]Average of all the H_2O ligands, on a single configuration (CP-opt; reoptimization of BLYP/SDD geometries). No second shell Cl^- counterions are included. [b]Average of all H_2O ligands and over the last picosecond of CPMD (50 snapshots). All system are neutralized by the required amount of Cl^- counterions, present in the second shell. [c]Individual water molecule in the gas phase, acetonitrile and water; values from references 4a, 4b, and 62, respectively. [d]In square brackets: without second-shell Cl^- (+3 charged system). [e]Average dipole moment of the three second shell H_2O molecules: 2.61(22) D.

Table 3. Atomic Charges (in e) from Natural Population Analysis[a]

	La	O	H_2O[b]	Cl
0.9.0	1.72	−0.91	0.14	
1.8.0	1.39	−0.90	0.14	−0.50
2.7.0	1.12	−0.89	0.14	−0.54
3.6.0	0.97	−0.87	0.14	−0.61
0.8.0	1.86	−0.93	0.14	
1.7.0	1.50	−0.91	0.14	−0.44
2.6.0	1.21	−0.90	0.13	−0.50
3.5.0	1.03	−0.88	0.13	−0.56

[a]BLYP/SDD(+) level on gas-phase BLYP/SDD geometries; for seven-coordinate complexes and Mulliken charges see Supporting Information, Table S3. [b]Sum of H and O atoms.

dx.doi.org/10.1021/ic302255a | Inorg. Chem. 2012, 51, 13396−13407

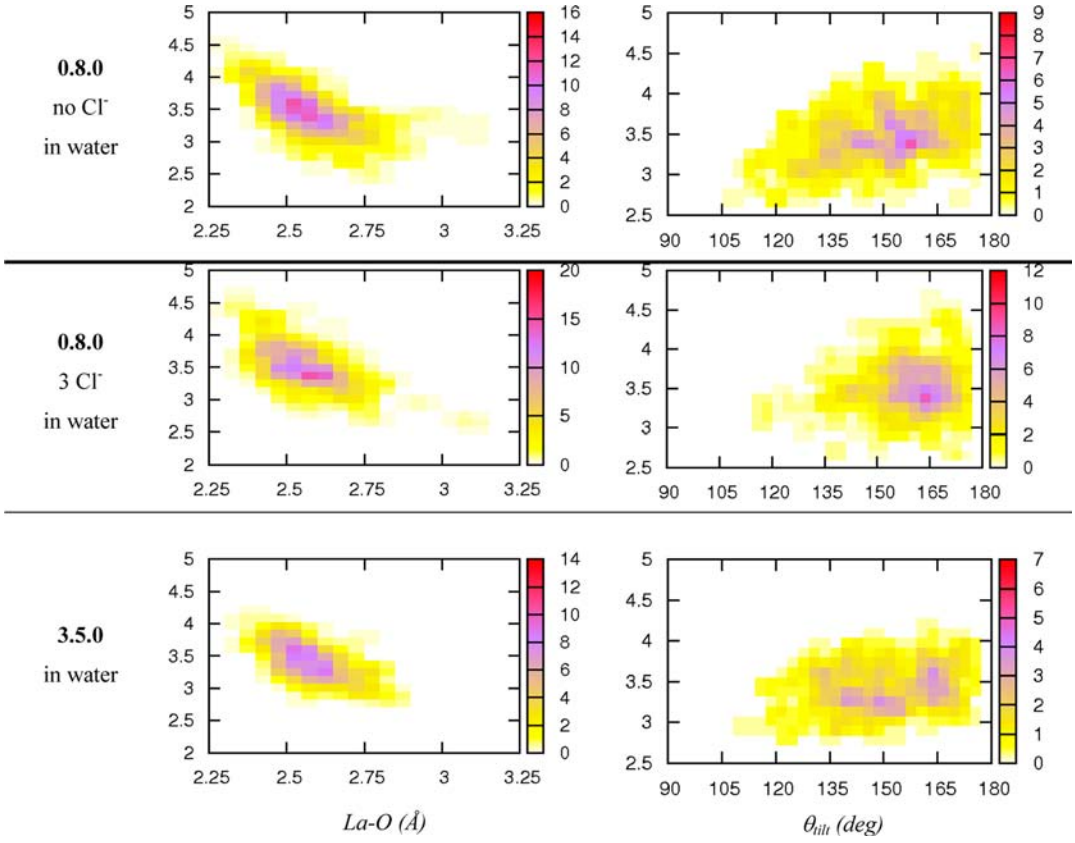

Figure 3. Scatter plots of the dipole moments of aquo ligands vs selected geometrical parameters along CPMD trajectories in water: results are shown as density maps in rectangular bins, (color-coded according to occurrences over 50 snapshots during the last ps of MD). See Supporting Information, Scheme S1 for the definition of θ_{tilt}.

depends on the orientation of the H_2O ligands and is more effective when the water is close to the metal and untilted, rather than when it is more distant and tilted. The high mobility of aquo ligands (where La−O distances oscillate much and H_2O rotates) gives rise to the large standard deviations obtained in the $\langle\mu_{H2O}\rangle$ values in Table 2. That the tilt angles systematically deviates from 180° in all studied complex, regardless of the nature of the solvent may explain the weak extra polarization stemming from the solvent, in particular for the highly charged complexes **0.9.0** and **0.8.0** (Table 2). These have essentially the same μ_{H2O} throughout, but this stems from two opposing effects: The strong La−H_2O polarization in the pristine complexes (gas phase) is reduced in solution because of the more tilted orientation of the aquo ligands; however, this is compensated for by the extra polarization from the surrounding solvent (see for instance **0.8.0** in the gas vs MeCN, Supporting Information, Figure S4).

This analysis is complicated by the presence of the counterions. Closer inspection of the results for **0.8.0** in Figure 3 indicates that the presence of chloride ions in the second solvation shell not only serves to "contain" the water ligands in the first shell (i.e., escapes to distances beyond 3 Å are less frequent, in accordance with the simulations for **0.9.0** discussed above) but also tends to reduce the tilt angle somewhat (compare top right and middle right plot in Figure 3).[66] The presence of Cl^- ligands in the first coordination sphere seems to flatten the distribution of tilt angles, but without pronounced effect on the overall average (compare top right and bottom right plot in Figure 3).

Illustrative snapshots are shown in Figure 4, providing an impression of the extent of tilting for the different species in the different environments. Some bias in selecting such snapshots notwithstanding, it is apparent that, for instance, **0.8.0** or **0.9.0** with counterions (top of Figure 4) have a less pronounced tendency for tilted aquo ligand than, for example, **3.5.0** (see rightmost water molecule in the bottom left structure in Figure 4). The mean geometrical parameters describing this tilt are collected in Supporting Information, Table S4.

Cooperative polarization effects should also occur in humid, chloride-based ILs, where water may compete with the solvent anions for coordination to the metal cations.[67] In such a case, both first- and second- shell Cl^- anions can be present and affect the induced polarization effects. To explore this question, we also simulated **3.5.0** in an ionic liquid, [dmim]Cl (Table 1).[68,69] Because of the large box size, only a short run of 1.2 ps was accomplished. Though arguably too short for proper equilibration of the dynamical properties, this should be sufficient for a qualitative description of the dipole moments. During the last 0.8 ps and over 13 snapshots, the mean dipole moment of the water ligands was 3.30(42) D, that is, between the values in water and acetonitrile (Table 2). Thus, in terms of their capability to polarize ligands, chloride-based ILs do not appear to be special compared to conventional solvents. This finding is somewhat counterintuitive (because an M^{n+}-O(H)-H···Cl^- array as in the lower middle structure in Figure 4 might have been expected to induce a stronger polarization than, for example, M^{n+}-O(H)-H···OH_2), but is consistent with the insensitivity of $\langle\mu_{H2O}\rangle$ in **0.8.0** toward the presence or absence

dx.doi.org/10.1021/ic302255a | Inorg. Chem. 2012, 51, 13396−13407

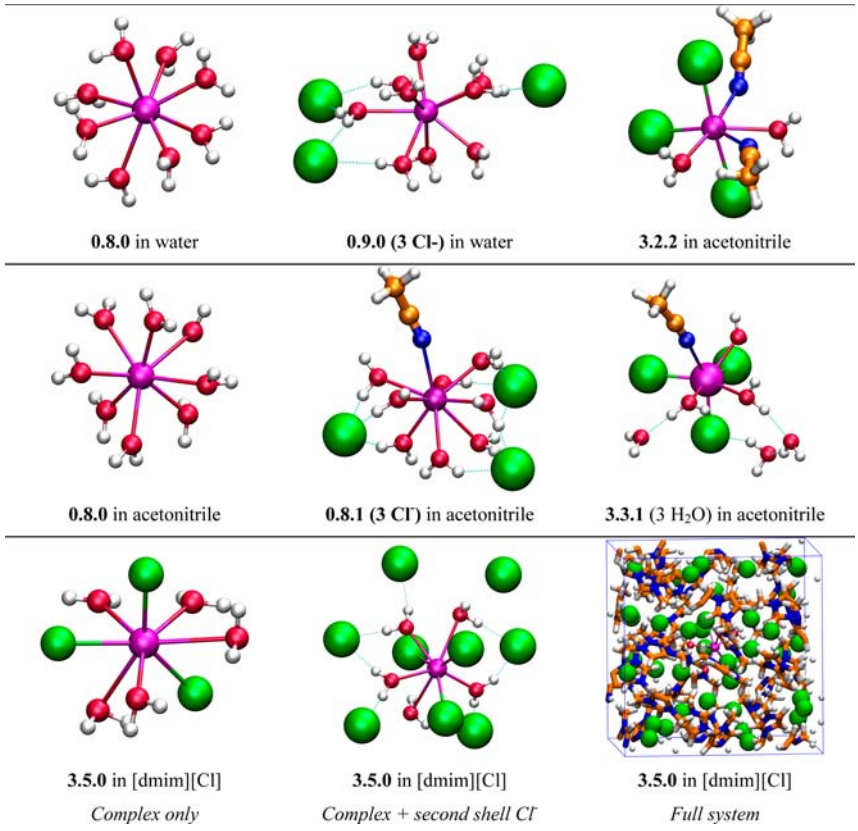

Figure 4. Typical snapshots of complexes in explicit acetonitrile, water and [dmim][Cl]. Dashed blue lines indicate the H_{H2O} atoms that are oriented toward counterions, the other ones interact with the solvent (hidden for clarity). In acetonitrile, aquo ligands are solvated by second shell H_2O molecules (if any) and acetonitrile molecules, see Supporting Information, Figure S3 for the case of **3.2.2**.

of chloride counterions in the second coordination sphere (Table 2).

3.3. Static Computations. We now assess the relative stability of selected water vs acetonitrile chloro complexes via energies for cumulative ligand displacement reactions obtained from static optimizations in the gas phase and solvation and free-energy corrections. At this point, some of the limitations of this methodology should be recalled. Besides shortcomings inherent in the BLYP functional (which for instance tends to overestimate metal−ligand bond distances significantly[70]) there are uncertainties in the computed free energies, because entropic contributions in solution are notoriously difficult to model with the underlying ideal-gas/harmonic-oscillator approximation, in particular for dissociative processes.[71] The simple continuum model applied[72] may also entail notable errors, especially for reaction energies involving free chloride (eq 3) and the associated huge differential solvation effects.

As we are, thus, now mainly interested in global trends, no extensive search for stereoisomers was undertaken. Rather, the anionic chloro ligands were placed as far apart of each other as possible, affording the structures shown schematically in Scheme 1.

First, in context with the constrained CPMD simulations discussed in section 3.1, chloride affinities are evaluated according to

$$[La(H_2O)_y]^{3+} + xCl^- \rightarrow [La(H_2O)_{y-x}Cl]^{3-x} + xH_2O; \quad (x = 1, 2, 3,\ y = 7, 8, 9) \qquad (3)$$

The results are summarized in Table 4. As expected, the metal binds chloride better in acetonitrile than in water and when fewer other coligands are present. The first entry ($x = 1$, $y = 9$, ΔG = 5.4 kcal/mol) can be compared to the free energy of chloride binding according to the CPMD value discussed above

Table 4. Reaction Free Energies (kcal/mol) for the Exchange of x H_2O by x Cl^- Ligands from $[La(H_2O)_y]^{3+}$ (0.9.0 - 0.7.0) According to eq 3, in the Gas Phase (ΔG Gas) and in Solution (ΔG PCM)[a]

	ΔG gas	ΔG PCM	ΔG PCM
reaction	gas	aceto nitrile	water
Ninefold Coordinated Complexes			
0.9.0 + 1 Cl^- → **1.8.0** + 1 H_2O	−254.7	1.4	5.4
0.9.0 + 2 Cl^- → **2.7.0** + 2 H_2O	−438.3	−3.9	4.4
0.9.0 + 3 Cl^- → **3.6.0** + 3 H_2O	−548.6	−2.9	2.5
Eightfold Coordinated Complexes			
0.8.0 + 1 Cl^- → **1.7.0** + 1 H_2O	−263.6	−5.7	−0.8
0.8.0 + 2 Cl^- → **2.6.0** + 2 H_2O	−448.6	−6.8	0.1
0.8.0 + 3 Cl^- → **3.5.0** + 3 H_2O	−561.0	−6.9	1.6
Sevenfold Coordinated Complexes			
0.7.0 + 1 Cl^- → **1.6.0** + 1 H_2O	−274.3	−10.2	−7.3
0.7.0 + 2 Cl^- → **2.5.0** + 2 H_2O	−466.9	−18.8	−11.6
0.7.0 + 3 Cl^- → **3.4.0** + 3 H_2O	−579.9	−17.0	−9.6

[a]BLYP/SDD/6-311+G** single point energies on BLYP/SDD/6-31G** gas phase optimized structures. See Supporting Information, Table S5 for thermodynamic and BSSE corrections.

dx.doi.org/10.1021/ic302255a | Inorg. Chem. 2012, 51, 13396−13407

Table 5. Reaction Free Energies (kcal/mol) for the Exchange of All H_2O Ligands by MeCN Ligands in Aquo Complexes[a]

reaction	ΔG gas	ΔG PCM	ΔG PCM	ΔG water
	gas	acetonitrile	water	per ligand[b]
Ninefold Coordinated Complexes				
0.9.0 + 9 MeCN → **0.9.0** + 9 H_2O	−113.8	33.4	37.7	4.2
1.8.0 + 8 MeCN → **1.0.8** + 8 H_2O	−51.4	22.4	25.7	3.2
2.7.0 + 7 MeCN → **2.0.7** + 7 H_2O	−1.6	24.9	24.9	3.6
3.6.0 + 6 MeCN → **3.0.6** + 6 H_2O	31.8	19.1	20.9	3.5
Eightfold Coordinated Complexes				
0.8.0 + 8 MeCN → **0.0.8** + 8 H_2O	−116.5	29.5	33.4	4.2
1.7.0 + 7 MeCN → **1.0.7** + 7 H_2O	−55.7	19.5	22.1	3.2
2.6.0 + 6 MeCN → **2.0.6** + 6 H_2O	−14.1	9.6	11.8	2.0
3.5.0 + 5 MeCN → **3.0.5** + 5 H_2O	*dissoc*[c]	*dissoc*[c]	*dissoc*[c]	
Sevenfold Coordinated Complexes				
0.7.0 + 7 MeCN → **0.0.7** + 7 H_2O	−120.3	24.9	25.8	3.7
1.6.0 + 6 MeCN → **1.0.6**[d] + 6 H_2O	−59.5	17.8	21.6	3.6
2.5.0 + 5 MeCN → **2.0.5** + 5 H_2O	−15.9	10.6	11.2	2.2
3.4.0 + 4 MeCN → **3.0.4** + 4 H_2O	9.9	3.0	5.0	1.3

[a]According to eqs 4. Values computed in the gas phase (ΔG Gas) and in solution (ΔG PCM). BLYP/SDD/6-311+G** single point energies on BLYP/SDD/6-31G** gas phase optimized structures. See Supporting Information, Table S6 for thermodynamic and BSSE corrections. [b]ΔG PCM water value divided by the number of water ligands. [c]One acetonitrile ligand dissociated from **3.0.5** during the optimization. [d]Pentagonal bipyramidal structure with axial Cl.

(eq 2, ΔA = 2.6 kcal/mol) and to experiment (ΔG^0 = 2.0 kcal/mol). Despite the methodological limitations just discussed, the overall qualitative agreement between all these numbers is rather good.

Next, the relative affinities toward water and acetonitrile as a function of chloride content are assessed through the following reactions:

$$[LaCl_x(H_2O)_y]^{3-x} + y\text{MeCN} \rightarrow [LaCl_x(\text{MeCN})_y]^{3-x} + yH_2O \qquad (x = 1\text{–}3,\ x + y = 7\text{–}9) \qquad (4)$$

According to the data collected in Table 5, acetonitrile is intrinsically (i.e., in the gas phase) favored over water for all cationic complexes, wheras it is the other way around for the neutral complexes (i.e., x = 3), similar to what had been found for related uranyl species.[4] In collision experiments in a mass spectrometer, it is indeed very difficult to replace acetonitrile ligands in **0.0.8** by water.[18] The preference for H_2O binding over MeCN increases with the amount of coordinated Cl^-, and this behavior can be rationalized by the formation of intramolecular hydrogen bonds between aquo and chloro ligands in the first coordination sphere. This feature can be seen on geometrical data reported in Supporting Information, Table S4, where H_2O exhibits very large tilt angles (e.g., 116° in **3.5.0**) resulting from attractive $Cl^-\cdots HOH\cdots Cl^-$ interactions. A similar feature has been obtained in the case of $[UO_2Cl_3L]^-$ (L = H_2O vs MeCN).[4b]

In solution, water is indicated to be the better ligand throughout, again as found for uranyl.[4] Normalized per entering water ligand (for aqueous solution see last column in Table 5), the driving force for displacement decreases with increasing chloride content, with decreasing coordination number, and on going from aqueous to acetonitrile solution. Thus, only a weak preference of **3.4.0** over **3.0.4** is computed in acetonitrile, namely, 3.0 kcal/mol (Table 5), that is, less than 1 kcal/mol per neutral ligand. This small value is certainly within the uncertainty of the methodology employed, and can still be regarded as compatible with the CPMD simulation of **3.4.0** in explicit acetonitrile, where one water ligand was exchanged spontaneously against a solvent molecule to afford **3.3.1** (Figure 2).

Finally, selected ligand binding energies were evaluated (see Table 6 for water ligands). Unlike the reactions discussed so far, in which the coordination number about La was preserved, such dissociation energies may suffer from the general tendency of standard density functionals to underestimate metal–ligand bond strengths.[51] For both **0.9.0** and **3.6.0**, the first water is rather weakly bound in solution. This result is in qualitative accord with the CPMD simulations discussed above, where this ligand is essentially unbound (cf. ΔA = −0.7 kcal/mol for ligand dissociation from **0.9.0** in water, Figure 1, and spontaneous water dissociation from **3.6.0** in acetonitrile, Figure 2). Dissociation of the next water ligand is indicated to be more difficult than the first one for the hydrate (compare first and second row in Table 6), but easier for the trichloro species (compare third and fourth row). This finding, which is consistent with the spontaneous formation of **3.4.0** from **3.6.0** in acetonitrile (Figure 2), is probably related to the better solvation of the less symmetrical **3.4.0** with its higher dipole moment. In water (PCM), the dipole moments of the complexes effectively increases in the following order **3.6.0** (0.11 D) < **3.5.0** (2.88 D) < **3.4.0** (3.88 D).

Table 6. Selected Free Energies (kcal/mol) for the Dissociation of H_2O Ligands[a]

	gas	acet.	water
	ΔG_{gas}	ΔG_{PCM}	ΔG_{PCM}
0.9.0 → **0.8.0** + H_2O	14.0	3.4	2.4
0.8.0 → **0.7.0** + H_2O	20.4	6.2	6.8
3.6.0 → **3.5.0** + H_2O	1.8	−0.4	1.7
3.5.0 → **3.4.0** + H_2O	1.5	−3.8	−4.4

[a]Values computed in the gas phase (ΔG Gas) and in solution (ΔG PCM). BLYP/SDD/6-311+G** single point energies on BLYP/SDD/6-31G** gas phase optimized structures. See Supporting Information, Table S7 for thermodynamic and BSSE corrections.

dx.doi.org/10.1021/ic302255a | Inorg. Chem. 2012, 51, 13396–13407

When the water-chloride displacement and water dissociation energies (including those from Tables 4 and 6) are combined into a "speciation diagram", **2.5.0** is obtained as the lowest free energy minimum in both aqueous and nonaqueous solution (see Supporting Information, Table S8 and Figure S6). Because this finding is clearly at odds with experimental observations in water, it will not be discussed further.

4. CONCLUSION

Absolute and relative binding energies of chloride, water, and acetonitrile ligands with La^{3+} have been studied in aqueous and acetonitrile solution, using a combination of static and dynamic DFT methods. La^{3+} strongly prefers MeCN over water as a ligand in the gas phase if less than three chlorides are coordinated. Otherwise, and especially for the static minima in a polarizable continuum, water is computed to bind more strongly than MeCN. The presence of chloride in the coordination sphere of La affects the binding of other ligands, arguably through the significant charge transfer from chloride to lanthanum in the mixed complexes. Very likely, the tendency toward lower coordination numbers with increasing chloride content is driven by this charge transfer. The affinity of La^{3+} toward chloride is much reduced on going from water to acetonitrile as solvent. All these findings are in qualitative agreement with experimental observations, but quantitative prediction of the speciation in this complex system remains a challenge. For instance, the trichloro complex in acetonitrile appears to be a borderline case: Predicted to be seven-coordinate in this medium, static PCM calculations slightly favor water over MeCN coordination, whereas a spontaneous exchange of water by MeCN is observed in a CPMD simulation. Static PCM results also favor, erroneously, $[LaCl_2(H_2O)_5]^+$ as the global minimum in aqueous solution.

Quantitative modeling of speciation is likely to require free-energy simulations with explicit solvent. We have opened the way into that direction with the first CPMD simulations reproducing the known chloride binding energy of $[La(H_2O)_9]^{3+}$. Explicit inclusion of counterions in the second solvation sphere and the bulk has been shown to be crucial. The success of this technique for 5f complexes (i.e., uranyl)[32] thus appears to carry over to 4f compounds as well. Short unconstrained CPMD simulations have been performed for selected mixed complexes in water and acetonitrile, to probe for spontaneous processes that would inform on structural and energetic preferences. The results provide evidence that seven- or eight-coordination is preferred for mixed $La^{3+}/H_2O/MeCN/Cl^-$ complexes in MeCN, in qualitative overall agreement with the static PCM computations.

Attempts to rationalize these findings through the extent of cooperative polarization of water ligands have met variable success. For uranyl complexes, immersion into a polar solvent had been found to increase the dipole moment of water ligands by about 1 D, almost irrespective of the other coligands.[4] For the La^{3+} complexes, this "extra" polarization is much more variable, decreasing with the chloride content and essentially vanishing for the binary aquo complexes, $[La(H_2O)_n]^{3+}$ (n = 8,9). As a consequence, very similar water dipole moments are obtained for all La complexes studied, around about 3.5 and 3.2 D in water and acetonitrile solution, respectively (and in between for a model ionic liquid, [dmim]Cl). The extent of extra polarization has been traced back to the fluctuations of key structural parameters during the MD, and turned out to be more pronounced at shorter La−O distances and smaller La−OH_2 tilts. This possible link between structural dynamics and electrostatic interactions, which are at the heart of ion solvation in polar solvents, is intriguing and deserves further scrutiny.

■ ASSOCIATED CONTENT

Supporting Information

Additional graphical and tabular material, full citations of refs 35 and 36, as well as optimized coordinates of the complexes of this study. This material is available free of charge via the Internet at http://pubs.acs.org.

■ AUTHOR INFORMATION

Corresponding Author

*Fax: (+44)(0)1334 463808. E-mail: buehl@st-andrews.ac.uk.

Notes

The authors declare no competing financial interest.

■ ACKNOWLEDGMENTS

This work was supported by EaStChem via the EaStChem Research Computing facility and a local Opteron PC cluster maintained by Dr. H. Früchtl. N.S. thanks the UJF and the CNRS for funding and the CECIC for computer resources. A.C. and W.G. are grateful to IDRIS, CINES, the Université de Strasbourg, as well as GDR CNRS PARIS for computer resources.

■ REFERENCES

(1) Review: Mincher, B. J.; Modolo, G.; Mezyk, S. P. *Solvent Extr. Ion Exch.* **2010**, *28*, 415−436.

(2) For modeling studies see for example: (a) Benay, G.; Schurhammer, R.; Wipff, G. *Phys. Chem. Chem. Phys.* **2011**, *13*, 2922−2934. Review: (b) Lan, J. H.; Shi, W. Q.; Yuan, L. Y.; Li, J.; Zhao, Y. L.; Chai, Z. F. *Coord. Chem. Rev.* **2012**, *256*, 1406−1417.

(3) Review of structural and thermodynamical properties of Ln complexes in nonaqueous solvents: Di Bernardo, P.; Melchior, A.; Tolazzi, M.; Zanonato, P. *Coord. Chem. Rev.* **2012**, *256*, 328−351.

(4) (a) Bühl, M.; Sieffert, N.; Chaumont, A.; Wipff, G. *Inorg. Chem.* **2011**, *50*, 299−308. (b) Bühl, M.; Sieffert, N.; Chaumont, A.; Wipff, G. *Inorg. Chem.* **2012**, *51*, 1943−1952.

(5) Review: Smirnov, P. R.; Trostin, V. N.; Russ., J. *Gen. Chem.* **2012**, *82*, 360−378.

(6) In the Cambridge Structure Database alone, 11 such structures are deposited (CSD version 5.33, May 2012).

(7) There are at least two clathrate structures, however, containing eight-coordinate $[La(H_2O)_8]^{3+}$: (a) Hardie, M. J.; Raston, C. I.; Salinas, A. *Chem. Commun.* **2001**, 1850. CSD refcode VOGJOQ, with a bulky carborane counteranion (b) Dong, Y.-B.; Wang, P.; Ma, J.-P.; Zhao, X.-X.; Wang, H.-Y.; Tang, B.; Huang, R.-Q. *J. Am. Chem. Soc.* **2007**, *129*, 4872 , refcode XIDZEQ, with a bulky La(III) acetato complex and free chloride as counterions.

(8) Ikeda, T.; Hirata, M.; Kimura, T. *J. Chem. Phys.* **2005**, *122*, 244507.

(9) Terrier, C.; Vitorge, P.; Gaigeot, M.-P.; Spezia, R.; Vuilleumier, R. *J. Chem. Phys.* **2010**, *133*, 044509.

(10) Lutz, O. M. D.; Hofer, T. S.; Randolf, B. R.; Rode, B. M. *Chem. Phys. Lett.* **2012**, *536*, 50−54.

(11) For example: (a) Duvail, M.; Souaille, M.; Spezia, R.; Cartailler, T.; Vitorge, P. *J. Chem. Phys.* **2007**, *127*, 034503.

(12) Rutkowski, P. X.; Michelini, M. C.; Gibson, J. K. *Phys. Chem. Chem. Phys.* **2012**, *14*, 1965−1977.

(13) Diaz-Moreno, S.; Ramos, S.; Bowron, D. T. *J. Phys. Chem. A* **2011**, *115*, 6575−6581.

(14) Allen, P. G.; Bucher, J. J.; Shuh, D. K.; Edelstein, N. M.; Craig, I. *Inorg. Chem.* **2000**, *39*, 595−601.

(15) Petit, L.; Vuilleumier, R.; Maldivi, P.; Adamo, C. *J. Phys. Chem. B* **2008**, *112*, 10603−10607.

(16) Wasse, J. C.; Salmon, P. S. *J. Phys.: Condens. Matter* **1999**, *11*, 1381−1396.
(17) Glover, W. J.; Madden, P. A. *J. Chem. Phys.* **2004**, *121*, 7293−7303.
(18) Shi, T.; Hopkinson, A. C.; Siu, K. W. M. *Chem.—Eur. J.* **2007**, *13*, 1142−1151.
(19) (a) Deacon, G. B.; Gortler, B.; Junk, P. C.; Lork, E.; Mews, R.; Petersen, J.; Zemva, B. *J. Chem. Soc., Dalton Trans.* **1998**, 3887. (AsF_6^- counterions), for other early lanthanides see: (b) Bodizs, G.; Raabe, I.; Scopelliti, R.; Krossing, I.; Helm, L. *Dalton Trans.* **2009**, 5137−5147.
(20) Baaden, M.; Berny, F.; Madic, C.; Wipff, G. *J. Phys. Chem. A* **2000**, *104*, 7659−7671.
(21) For example: (a) Chaumont, A.; Wipff, G. *Inorg. Chem.* **2009**, *48*, 4277−4289. (b) Binnemans, K. *Chem. Rev.* **2007**, *107*, 2592−2614.
(22) For example, for extraction of nuclear waste: Sun, X. Q.; Luo, H. M.; Dai, S. *Chem. Rev.* **2012**, *112*, 2100−2128.
(23) See for example: (a) Bünzli, J. C. G.; Merbach, A. E.; Nielson, R. M. *Helv. Chim. Acta* **1987**, *139*, 151−152. (b) Bünzli, J. C. G.; Milicic-Tang, A. *Inorg. Chim. Acta* **1996**, *252*, 221−228. See also: (c) Bünzli, J. C. G.; Milicic-Tang, A. Solvation and anion interaction in organic solvents. In *Handbook on the Physics and Chemistry of Rare Earths*; Gschneidner, K. A., Jr., Eyring, L., Eds.; Elsevier: Amsterdam, The Netherlands, 1995; Vol. *21*, Chapter 145, pp 305−366.
(24) (a) Becke, A. D. *Phys. Rev. A* **1988**, *38*, 3098−3100. (b) Lee, C.; Yang, W.; Parr, R. G. *Phys. Rev. B* **1988**, *37*, 785−789.
(25) Cao, X.; Dolg, M. *J. Chem. Phys.* **2001**, *115*, 7348−7355.
(26) Martin, R. L.; Hay, P. J.; Pratt, R. L. *J. Phys. Chem. A* **1998**, *102*, 3565.
(27) As implemented in Gaussian 03: (a) Barone, V.; Cossi, M.; Tomasi, J. *J. Comput. Chem.* **1998**, *19*, 404−417. (b) Cossi, M.; Scalmani, G.; Rega, N.; Barone, V. *J. Chem. Phys.* **2002**, *117*, 43−54. (c) Cossi, M.; Crescenzi, O. *J. Chem. Phys.* **2003**, *19*, 8863−8872.
(28) (a) Krishnan, R.; Binkley, J. S.; Seeger, R.; Pople, J. A. *J. Chem. Phys.* **1980**, *72*, 650−654. (b) Clark, T.; Chandrasekhar, J.; Spitznagel, G. W.; Schleyer, P. v. R. *J. Comput. Chem.* **1983**, *4*, 294−301.
(29) Ho, J.; Klamt, A.; Coote, M. L. *J. Phys. Chem. A* **2010**, *114*, 13442−13444.
(30) In Gaussian 03 E_{solv}, the SCF energy without the non-electrostatic terms, is printed as ⟨psi(f)|H+V(f)/2|psi(f)⟩ under "Variational PCM results".
(31) Boys, S. F.; Bernardi, F. *Mol. Phys.* **1970**, *19*, 553.
(32) For a review see: Bühl, M.; Wipff, G. *ChemPhysChem* **2011**, *12*, 3095−3105.
(33) The initial CPMD/BLYP simulations in the Parrinello group have afforded good descriptions of liquid water, see for instance: (a) Sprik, M.; Hutter, J.; Parrinello, M. *J. Chem. Phys.* **1996**, *105*, 1142−1152. Although potential shortcomings of this functional are now better appreciated, see: (b) Van deVondele, J.; Mohamed, F.; Krack, M.; Hutter, J.; Sprik, M.; Parrinello, M. *J. Chem. Phys.* **2005**, *122*, 014515 , and references cited therein.
(34) Reed, A. E.; Curtiss, L. A.; Weinhold, F. *Chem. Rev.* **1988**, *88*, 899−926.
(35) Frisch, M. J.; Pople, J. A.; et al. *Gaussian 03*, Revision E.01; Gaussian, Inc.: Pittsburgh, PA, 2003.
(36) Frisch, M. J.; et al. *Gaussian 09*, Rev. A.02; Gaussian, Inc.: Wallingford, CT, 2009; this was done because it had been noted that Gaussian 03 does not use the proper valence/Rydberg partitioning scheme for f-elements: Clark, A. E.; Sonnenberg, J. L.; Hay, P. J.; Martin, J. L. *J. Chem. Phys.* **2004**, *121*, 2563−2570.
(37) Car, R.; Parrinello, M. *Phys. Rev. Lett.* **1985**, *55*, 2471−2474.
(38) Troullier, N.; Martins, J. L. *Phys. Rev. B* **1991**, *43*, 1993−2006.
(39) Kleinman, L.; Bylander, D. M. *Phys. Rev. Lett.* **1982**, *48*, 1425−1428.
(40) Case, D. A.; Pearlman, D. A.; Caldwell, J. W.; Cheatham III, T. E.; Wang, J.; Ross, W. S.; Simmerling, C. L.; Darden, T. A.; Merz, K. M.; Stanton, R. V.; Cheng, A. L.; Vincent, J. J.; Crowley, M.; Tsui, V.; Gohlke, H.; Radmer, R. J.; Duan, Y.; Pitera, J.; Massova, I.; Seibel, G. L.; Singh, U. C.; Weiner, P. K.; Kollman, P. A. *AMBER7*, 7; University of California: San Fransisco, CA, 2002.
(41) Bühl, M.; Chaumont, A.; Schurhammer, R.; Wipff, G. *J. Phys. Chem. B* **2005**, *109*, 18591−18599.
(42) Gerkin, R. E.; Reppart, W. J. *Acta Crystallogr., Sect. C* **1984**, *40*, 781 (ethyl sulfate counterions, CSD refcode ZZZAQP01).
(43) Bühl, M.; Grigoleit, S.; Kabrede, H.; Mauschick, F. T. *Chem.—Eur. J.* **2006**, *12*, 477−488.
(44) Errington, W.; Spry, M. P.; Willey, G. R. *Acta Crystallogr., Sect. C.* **1998**, *54*, 290 (refcode NIDQAS).
(45) (a) Marzari, N.; Vanderbilt, D. *Phys. Rev. B* **1997**, *56*, 12847. (b) Silvestrelli, P. L.; Marrzari, N.; Vanderbilt, D.; Parrinello, M. *Solid State Commun.* **1998**, *107*, 7. Wannier functions are a generalization to infinite periodic systems of the Boys localized orbitals: (c) Boys, S. F. In *Quantum Theory of Atoms, Molecules, and the Solid State*; Löwdin, P.-O., Ed.; Academic Press: New York, 1966; p 253. Wannier centers are the maxima of these localized orbitals denoting the highest negative charge concentration. For a review with some more background on Wannier functions and centers see: (d) Tse, J. S. *Annu. Rev. Phys. Chem.* **2002**, *53*, 249−290.
(46) Sprik, M.; Ciccotti, G. *J. Chem. Phys.* **1998**, *109*, 7737−7744 , and references cited therein.
(47) CPMD Version 3.13.1, Copyright IBM Corp. 1990−2008, Copyright MPI für Festkörperforschung Stuttgart 1997−2001.
(48) After 0.5 ps pre-equilibration with all nine La-O distances fixed to the X-ray values.
(49) For further validation of the cutoff see the Supporting Information, Table S2.
(50) Given that La^{3+} has a negative limiting partial molar volume (Marcus, Y. *Ion Solvation*; Wiley: New York, 1985), a density of 1.0 would seem somewhat low for this simulation. However, using a slightly lower density can help to improve sampling and to maintain liquid-like behavior, especially since the "intrinsic" density of liquid water with the BLYP functional used here is but 0.9 at 323 K, see: McGrath, M. J.; Siepmann, J. I.; Kuo, I-F. W.; Mundy, C. J.; VandeVondele, J.; Hutter, J.; Mohamed, F.; Krack, M. *J. Phys. Chem. A* **2006**, *110*, 640−646.
(51) See for instance: Rotzinger, F. R. *J. Phys. Chem. B* **2005**, *109*, 1510−1527.
(52) Bühl, M.; Schreckenbach, G.; Sieffert, N.; Wipff, G. *Inorg. Chem.* **2009**, *48*, 9977−9979.
(53) 0.2 M solution ($CF_3SO_3^-$ counterions), in 0.1 M CF_3SO_3H: Persson, I.; D'Angelo, P.; De Panfilis, D.; Sandstrom, M.; Eriksson, L. *Chem.—Eur. J.* **2008**, *14*, 3056.
(54) The uncertainty was estimated from the largest standard deviation of the running average of ⟨*f*⟩ during the last ps of the constrained runs (see Supporting Information, Figure S1 for an illustrative example), multiplied with the total integration width. This uncertainty refers to the numerical precision of the PTI technique. The absolute uncertainty due to the accuracy of the underlying quantum-chemical methodology (density functional, pseudopotential, basis set) is, arguably, considerably higher.
(55) Even before this event, the structure of **1.8.0**·(**2Cl**$^-$) appeared rather labile, as instantaneous La-O distances approached and even shortly exceeded 3 Å (see the Supporting Information, Figure S1)
(56) Fernandez-Ramirez, E.; Jimenez-Reyes, M.; Solache-Rios, M. J. *J. Chem. Eng. Data* **2007**, *52*, 373−376.
(57) Bühl, M.; Sieffert, N.; Golubnychiy, V.; Wipff, G. *J. Phys. Chem. A* **2008**, *112*, 2428−2436.
(58) Soderholm, L.; Skanthakumar, S.; Wilson, R. E. *J. Phys. Chem. A* **2011**, *115*, 4959−4967.
(59) A number of seven-coordinate $LnCl_3(H_2O)_4$ complexes have also been characterized, for example, Ln = Er, Lu, Tm, Yb with co-crystallized 4-methylpyridinium chloride, see: (a) Semenova, L. I.; Skelton, B. W.; White, A. H. Z. *Anorg. Allg. Chem.* **2006**, *632*, 2405. In contrast La prefers eight-coordination in $[LaCl_4(H_2O)_4]^-$, see: (b) Ritchie, L. K.; Harrison, W. T. A. *Acta Crystallogr., Sect. E* **2006**, *62*, m1255.

(60) Also, taking the structures from CPMD snapshots as starting points for gas phase optimizations leads to isomers higher in energy than those depicted in Scheme 1 (even when considering PCM energies), because Cl^- ligands are too close to each other.
(61) This procedure affords a very simple point-charge model, where the positive atomic charges (screened by the core if present) are placed at the nuclear positions, and negative charges of −2 at the positions of the Wannier centers. The total dipole moment is then calculated from this distribution of point charges.
(62) See: Silvestrelli, P. L.; Parrinello, M. *J. Chem. Phys.* **1999**, *111*, 3572−3580 , and references cited therein.
(63) Molina, J. J.; Lectez, S.; Tazi, S.; Salanne, M.; Dufrêche, J.-F.; Roques, J.; Simoni, E.; Madden, P. A.; Turq, P. J. *Chem. Phys.* **2011**, *134*, 014511.
(64) PBE functional, CPMD and QM/MM-MD: Atta-Fynn, R.; Bylaska, E. J.; Schenter, G. K.; de Jong, W. A. *J. Phys. Chem. A* **2011**, *115*, 4665−4677.
(65) $\theta_{tilt} = 180°$ would correspond to coordination via the $2a_1$ ("sp^2"-type) lone pair of water; coordination via an sp^3 "rabbit ear" would occur at $\theta_{tilt} \approx 125°$. Alternatively, a tilt angle can also be defined as the angle between the La-O vector and the bisector of the HOH angle, which would correspond to $180° - \theta_{tilt}$.
(66) Tilt angles of aquo ligands from first-principles MD simulations in water have been discussed, but without taking counterions into account, for example, for aqueous La^{3+} and Cm^{3+} see references 9 and 64, respectively, for $[Gd(H_2O)_8]^{3+}$ see: Yazyev, O. V.; Helm, L. *J. Chem. Phys.* **2007**, *127*, 084506.
(67) See for example the cases of UO_2^{2+} and Eu^{3+} cations in humid [bmim][PF_6]: Chaumont, A.; Wipff, G. *Inorg. Chem.* **2004**, *43*, 5891.
(68) For CPMD simulations of the pristine IL see reference 41 (BP86 level) and Bhargava, B. L.; Balasubramanian, S. *Chem. Phys. Lett.* **2006**, *417*, 486−491.
(69) This system is intended as a model containing both chloride and aquo ligands and is not necessarily representative of the actual species present under experimental conditions; for example La^{3+} salts in ILs with chloride anions tend to form ate complexes such as $[LaCl_6]^{3-}$.
(70) Bühl, M.; Reimann, C.; Pantazis, D. A.; Bredow, T.; Neese, F. *J. Chem. Theory Comput.* **2008**, *4*, 1449−1459.
(71) The ad hoc pressure correction from reference 26 may not be a panacea, even though it has been shown to work well in certain cases, for example, Sieffert, N.; Bühl, M. *Inorg. Chem.* **2009**, *48*, 4622−4624.
(72) PCM results can also be very sensitive to methodological details, in particular the definition of the cavity: Wahlin, P.; Schimmelpfennig, B.; Wahlgren, U.; Grenthe, I.; Vallet, V. *Theor. Chem. Acc.* **2009**, *124*, 377−384 . We have chosen the particular PCM variant and cavity definition (default in Gaussian 03) for compatibility with our previous studies.